Physics Letters A 557 (2025) 130867

Contents lists available at ScienceDirect

Physics Letters A

journal homepage: www.elsevier.com/locate/pla

Letter

Measurement of the muon transfer rate from muonic hydrogen to carbon in the FAMU experiment

E. Mocchiutti [e], S. Monzani [e,f,*], C. Pizzolotto [e], A. Sbrizzi [c], A. Adamczak [a], D. Bakalov [b], G. Baldazzi [c,d], M. Baruzzo [e,f], R. Benocci [g,h], R. Bertoni [g], M. Bonesini [g,i], H. Cabrera [e,j], D. Cirrincione [e,f], M. Clemenza [g,i], L. Colace [k,l], M. Danailov [e,m], P. Danev [b], A. de Bari [n,o], E. Fasci [p,q], K.S. Gadedjisso-Tossou [e,j,s], L. Gianfrani [p,q], K. Ishida [t,u], A. Menegolli [n,o], L. Moretti [p,q], G. Morgante [r], A. Pullia [v,w], R. Ramponi [v,x], L.P. Rignanese [c], H.E. Roman [g,i], M. Rossella [o], R. Rossini [n,o], M. Stoilov [b], J.J. Suárez-Vargas [e,y], L. Tortora [k], E. Vallazza [g], A. Vacchi [e,f,t]

[a] Institute of Nuclear Physics, Polish Academy of Sciences, Radzikowskiego 152, PL31342 Kraków, Poland
[b] Institute for Nuclear Research and Nuclear Energy, Bulgarian Academy of Sciences, blvd. Tsarigradsko ch. 72, Sofia 1784, Bulgaria
[c] Sezione INFN di Bologna, viale Berti Pichat 6/2, Bologna, Italy
[d] Dipartimento di Fisica ed Astronomia, Università di Bologna, via Irnerio 46, Bologna, Italy
[e] Sezione INFN di Trieste, via A. Valerio 2, Trieste, Italy
[f] Dipartimento di Scienze Matematiche, Informatiche e Fisiche, Università di Udine, via delle Scienze 206, Udine, Italy
[g] Sezione INFN di Milano Bicocca, Piazza della Scienza 3, Milano, Italy
[h] Dipartimento di Scienze dell'Ambiente e della Terra, Università di Milano Bicocca, Piazza della Scienza 1, Milano, Italy
[i] Dipartimento di Fisica G. Occhialini, Università di Milano Bicocca, Piazza della Scienza 3, Milano, Italy
[j] The Abdus Salam International Centre for Theoretical Physics, Strada Costiera 11, Trieste, Italy
[k] Sezione INFN di Roma Tre, Via della Vasca Navale 84, Roma, Italy
[l] Dipartimento di Ingegneria Industriale, Elettronica e Meccanica, Università degli Studi Roma Tre, Via V. Volterra 62, Roma, Italy
[m] Sincrotrone Elettra Trieste, SS14, km 163.5, Basovizza, Italy
[n] Dipartimento di Fisica, Università di Pavia, via A. Bassi 6, Pavia, Italy
[o] Sezione INFN di Pavia, Via A. Bassi 6, Pavia, Italy
[p] Sezione INFN di Napoli, Via Cintia, Napoli, Italy
[q] Dipartimento di Matematica e Fisica, Università della Campania "Luigi Vanvitelli", Viale Lincoln 5, Caserta, Italy
[r] INAF-OAS Bologna, Area della Ricerca, via P. Gobetti 93/3, Bologna, Italy
[s] Laboratoire de Physique des Materiaux et des Composants à Semi-conducteurs (LPMCS), Département de physique, Université de Lomé, Lomé, Togo
[t] Riken Nishina Center, RIKEN, 2-1 Hirosawa, Wako, Saitama 351-0198, Japan
[u] Institute of Materials Structure Science, High Energy Accelerator Research Organization, 1-1 Oho, Tsukuba, Ibaraki 305-0801, Japan
[v] Sezione INFN di Milano, via Celoria 16, Milano, Italy
[w] Dipartimento di Fisica, Università degli Studi di Milano, via Celoria 16, Milano, Italy
[x] IFN-CNR, Dipartimento di Fisica, Politecnico di Milano, piazza Leonardo da Vinci 32, Milano, Italy
[y] INFN Laboratori Nazionali del Sud, Via S.Sofia 62, 95123 Catania, Italy

ARTICLE INFO

Communicated by S.-F. Ge

Keywords:
X-rays
$LaBr_3(Ce)$
Transfer rate
Carbon
Muonic atoms
Muonic hydrogen
Muonic X-rays

ABSTRACT

In 2016, the FAMU collaboration performed an experiment to measure the temperature dependence of the muon transfer rate from muonic hydrogen to different atoms (carbon, oxygen and argon). The results obtained with oxygen have been already published by the collaboration. This paper presents the results of the first measurement of the muon transfer rate to carbon as a function of the temperature in the range 197-300 K. The results suggest that oxygen is still the best candidate for the measurement of the Zemach radius of the proton with the FAMU experimental technique.

* Corresponding author at: Università di Udine, via Delle Scienze 206, Udine, Italy.
E-mail address: Simone.Monzani@uniud.it (S. Monzani).

https://doi.org/10.1016/j.physleta.2025.130867
Received 20 February 2025; Received in revised form 17 June 2025; Accepted 29 July 2025

Available online 7 August 2025

1. Introduction

The goal of the FAMU experiment is to extract the Zemach radius of the proton from a measurement of hyperfine splitting (hfs) of muonic hydrogen ground state (ΔE_{hfs}) [1].

In our experiment, muonic hydrogen is formed when a low momentum muon beam ($\approx$ 50 MeV/c) hits a cryogenic target contained in a high reflectivity optical cavity and filled with gaseous hydrogen. If a high-Z contaminant is added to hydrogen, there is a certain probability that the muon leaves muonic hydrogen to form an excited μZ atom (muon transfer process). The FAMU technique consists in illuminating the gaseous target with an intense and tunable laser beam at the time when muonic hydrogen is formed in the target. When the wavelength of the laser is tuned around the ΔE_{hfs} energy, the μp atoms will be excited from the lower singlet (F = 0) to the triplet state (F = 1). The μp atoms quickly de-excite from the triplet state back to the singlet state in collisions with the surrounding molecules, acquiring a kinetic energy up to 0.12 eV, which corresponds to temperatures of about 1000 K. If an increase in the transfer rate of muons from μp to Z atoms with rising energy is confirmed [2,3], then in muonic hydrogen that has gained kinetic energy through non-radiative de-excitation, the muon transfer rate to Z atoms will increase. This is signaled by the increase in the emission of muonic X-rays from the Z atoms if the spin-flip resonance wavelength is obtained. The challenge of the FAMU experiment is to design a sophisticated laser system that is precise, stable and powerful enough to produce a detectable increase of muon transfers around ΔE_{hfs}.

The variation of the muon transfer process as a function of temperature can be translated into a variation as a function of kinetic energy by convolving it with the Boltzmann distribution at each temperature. The resulting trend remains the same: kinetic energy increases with temperature. Moreover, the larger this variation, the more precisely the hyperfine splitting can be measured. Between 2016 and 2018, three experimental campaigns were carried out to study different aspects of the muon transfer process, without the use of the laser system. Different concentrations of oxygen, carbon and argon contaminants (mostly below 1%) were tested with the aim of finding the best target contaminant for the FAMU experiment, i.e. the element for which the transfer rate increases the most as the μp kinetic energy increases.

The results obtained with a H_2/O_2 gas mixture show that oxygen is a good candidate for the FAMU experiment because the muon transfer rate increases with the temperature in the range 70-336 K [4,5]. This paper presents the results obtained with a H_2/CH_4 gas mixture, complementing the previous work.

2. Experimental setup

The FAMU experiment is performed at the RIKEN-RAL facility [6] which provides a pulsed-muon beam with a repetition rate of 50 Hz. Each bunch consists of two gaussian spills of negative muons with a FWHM of about 70 ns and a time-separation of about 320 ns.

The target gas mixture is contained in a cryogenic aluminium vessel surrounded by eight X-rays detectors of the same type and size. Each detector unit is made of a Lanthanum Bromide scintillating crystal - $LaBr_3$(Ce) - one inch thick with a cylindrical shape. The best five $LaBr_3$(Ce) detectors with excellent energy resolution and efficiency, and having a very similar behavior and gain, were used in this data analysis.

Scintillation light signals are collected and amplified using Hamamatsu high speed photomultipliers (R11265U-200). The energy and the time associated to each electrical pulse is extracted from the digitized waveforms recorded with a 500 MHz CAEN V1730 digitizer.

A cooling system gives the possibility to vary the target temperature in a range from 30 K to room temperature. The muon beam and the details of the 2016 experimental setup are described in Ref. [7].

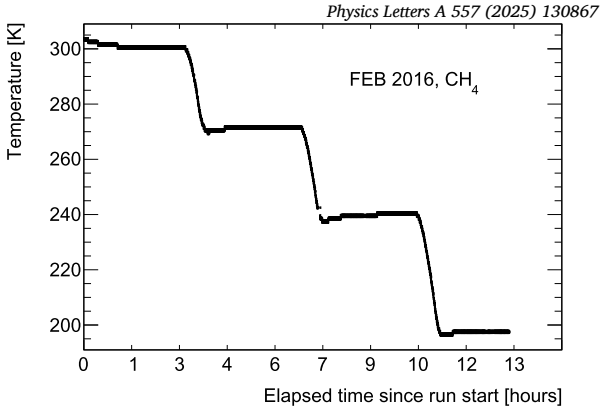

Fig. 1. The H_2/CH_4 target temperature as a function of time. Time is counted starting from the 25^{th} of February 2016 at about 9 pm.

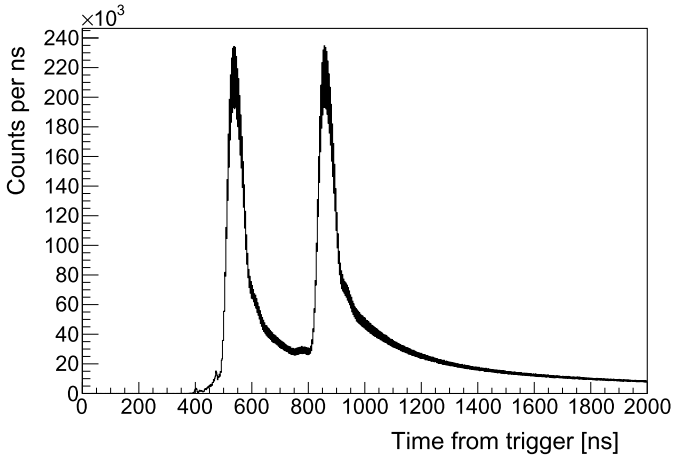

Fig. 2. Starting time of signals recorded with $LaBr_3$(Ce) detectors when muons are captured in the H_2/CH_4 target.

3. Data sample

The analysis presented in this paper is based on a data sample recorded in February 2016, when the cryogenic target was filled with a H_2/CH_4 mixture at 40 bar at room temperature. The CH_4 weight concentration in the mixture was 0.3%. The target was initially filled at room temperature and sealed. The temperature was then reduced in four steps (300 K, 270 K, 240 K and 197 K) corresponding to different pressure conditions of the air-tight target system. The lower limit of the temperature was constrained by the methan condensation temperature (191 K).

At each temperature, data were recorded for about three hours. During data-taking, the temperature was continuously monitored and kept constant with a precision of 0.5 K using four temperature sensors placed around the target. Fig. 1 shows the H_2/CH_4 target temperature as a function of time. Collected data amount to 1.4 M triggers.

A sample of 0.11 M triggers on a pure hydrogen target was collected in the same data taking period and it is used for background estimation.

4. Data analysis

The analysis technique used to extract the muon transfer rate from data is reported in Ref. [5], where the FAMU collaboration published the measurement of the muon transfer rate to oxygen. The same software package has been used to identify X-ray pulses, measure the associated energy and time stamp, and suppress the systematic effects due to the pile-up of adjacent signals.

Fig. 2 shows the starting time distribution (t_s) of X-rays passing the main selection criteria. The two peaks at about 540 ns and 860 ns cor-

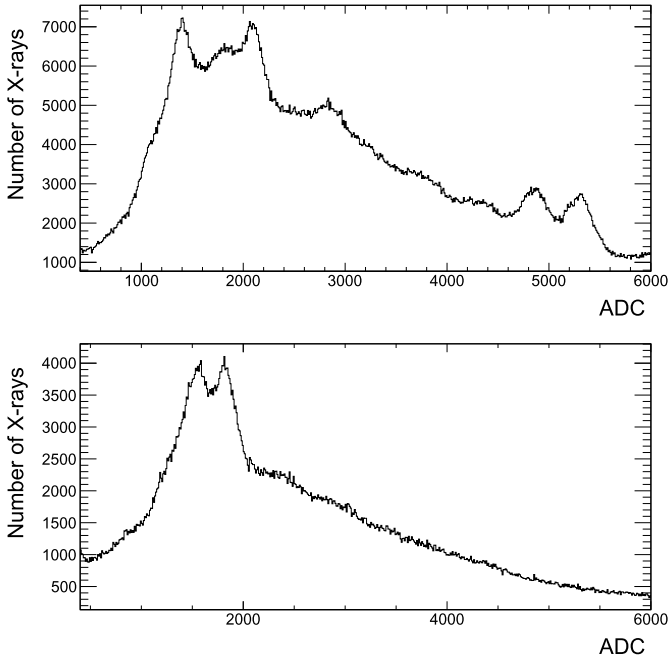

Fig. 3. Energy spectra measured with one $LaBr_3$(Ce) detector and a H_2/CH_4 target. The upper panel shows prompt X-rays with t_s in the range 490-590 ns and 810-910 ns. The lower panel shows delayed X-rays with t_s in the range 1600-4000 ns.

respond to the arrival time of the muon spills when a large number of prompt X-rays is produced by atoms present in the target material, i.e. mostly aluminium (65.8 keV, 88.8 keV, 346 keV) and nickel (107 keV, 309 keV). Delayed X-rays are produced by the carbon atoms contained in the gas mixture, hundreds of ns after the arrival of the muon spills. They correspond to the carbon K_α, K_β and K_γ lines at 75 KeV, 89 keV and 94 keV respectively. Fig. 3 shows the energy spectra for one of the $LaBr_3$(Ce) detectors for prompt and delayed X-rays (upper and lower panel respectively). The energy resolution of the K_α line of carbon ranges between 20% and 30%, depending on the given detector.

Fig. 4 shows the energy calibration done by fitting a second order polynomial to the points that relate the peak positions in ADC counts to the corresponding X-ray energies. The K_β and K_γ lines of carbon are excluded from the calibration fit because they are not resolved (they appear as a single peak in the lower panel of Fig. 3).

4.1. X-rays counting

The detection of delayed X-rays from carbon is the experimental signature of the muon transfer process from hydrogen to carbon. In order to evaluate the rate of muon transfers, the number of delayed X-rays is evaluated in a time window sufficiently separated from the prompt X-ray production region. The rate of prompt X-rays becomes negligible for $t_s > 1600$ ns, as well as the probability of having delayed X-rays for $t_s > 4000$ ns. Therefore, the optimal choice of delayed time window for this analysis is 1600 – 4000 ns.

The main source of background in the delayed time window is bremsstrahlung radiation from electrons emitted in muon decays. Such background is evaluated by recording X-ray pulses produced when the muon beam interacts with a pure H_2 target. Fig. 5 shows the energy spectrum of delayed X-rays recorded with all the available $LaBr_3$(Ce) detectors, before background subtraction (blue line). The H_2 spectrum used for background evaluation is also shown in Fig. 5 (red filled histogram).

The H_2 and H_2/CH_4 energy spectra are normalized in the range where the shapes are in good agreement, between 200 and 400 keV. The collected data sample of H_2 is about ten times smaller than the CH_4 one, leading to higher fluctuations in the energy spectrum. In the signal spectrum the tail at lower energy respect to the carbon K_α line is due to carbon X-rays depositing only a fraction of their energy in the crystals.

4.2. Transfer rate measurement

The muon transfer rate to carbon (Λ_{pC}) is extracted from the time dependent number of muon transfers to carbon after the thermalization of μp atoms. At a given temperature T, the number of μp atoms in the target ($N_{\mu p}$) changes with the time t according to the formula:

$$dN_{\mu p}(t) = -N_{\mu p}(t)\lambda_{dis}(T)dt. \quad (1)$$

The total disappearance rate of μp atoms, $\lambda_{dis}(T)$, can be expressed as:

$$\lambda_{dis}(T) = \lambda_0 + \phi[c_p\Lambda_{pp\mu} + c_d\Lambda_{pd}(T) + c_C\Lambda_{pC}(T)], \quad (2)$$

where λ_0 is the disappearance rate of the muons bound to protons, $\Lambda_{pp\mu}$ is the $pp\mu$ formation rate in μp collisions with hydrogen nuclei, Λ_{pd} is the muon transfer rate from μp to deuterium, Λ_{pC} is the muon transfer rate from μp to carbon atoms, ϕ is the atom density in the gaseous target, c_p, c_d, and c_C are the hydrogen, deuterium and carbon atomic concentrations in the target.

The set of constants used in this analysis is reported in Table 1.

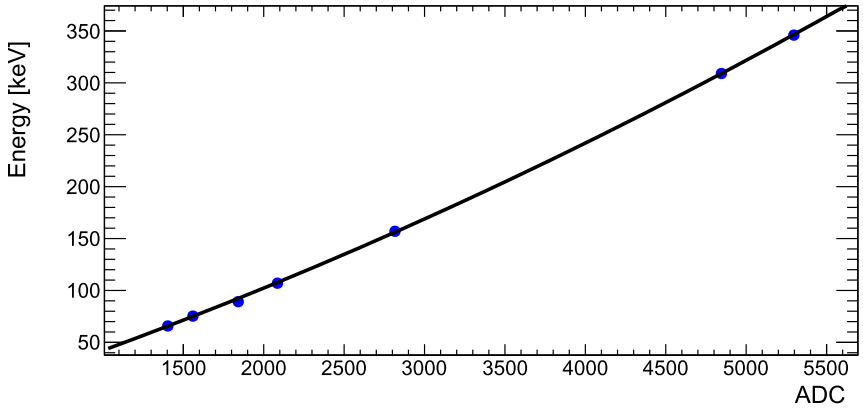

Fig. 4. Calibration curve of the $LaBr_3$(Ce) detector number 6. The horizontal error bar is estimated by varying the fitting range of a gaussian fit to the measured energy spectra around a given K line. The error bar is included in the marker size. The calibration curve is fitted with a second order polynomial function. The coefficients of the polynomial fit to the data points in increasing order are -11.2 ± 1.9, (5.02 ± 0.14)×10^{-2}, (3.4 ± 0.2)×10^{-6}.

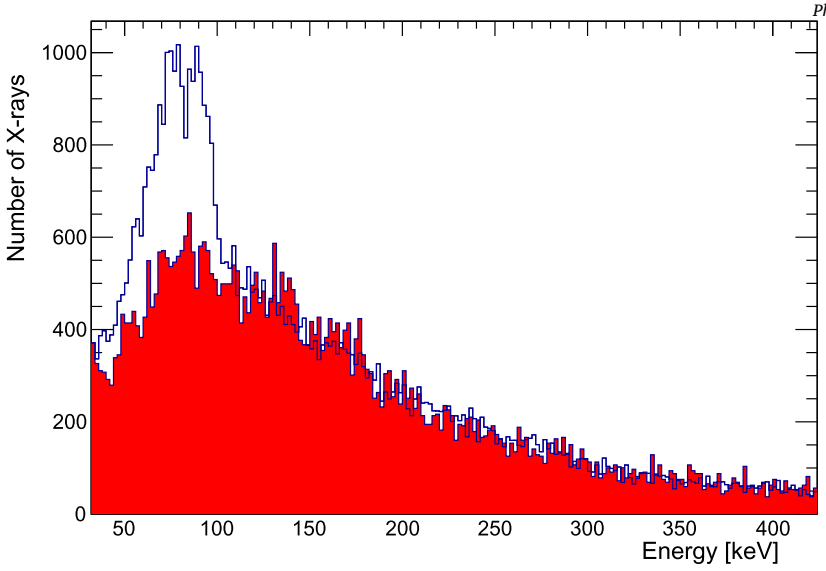

Fig. 5. Energy spectra of delayed X-rays produced in H_2/CH_4 (line) and H_2 (filled histo) with t_s in the time bin 2000-2190 ns as an example. Spectra are normalized in the range 200-400 keV.

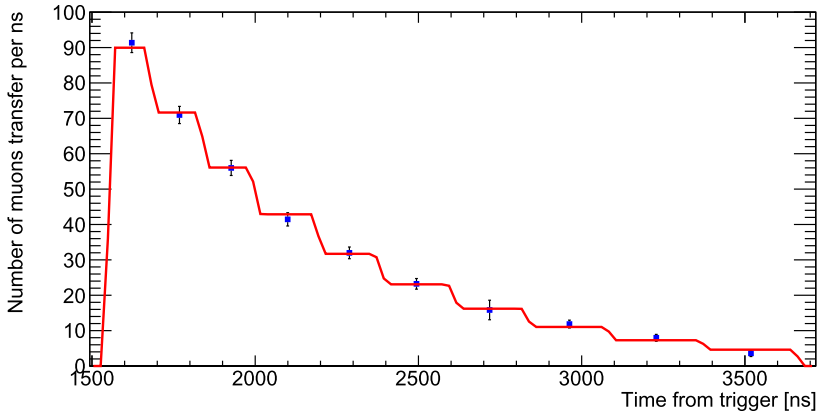

Fig. 6. Time dependence of the rate of muon transfers to carbon measured at 197 K. The error bars are the sum in quadrature of the statistical and the background-related systematic uncertainties. The fit to extract Λ_{pC} is superimposed.

Table 1
The values are derived from literature where indicated. The temperature dependence of Λ_{pd} has been taken into account in the fit. Concentrations are expressed as atomic concentrations and $c_p = 1. - c_d - c_C$. Carbon concentration and ϕ are derived directly from the experimental gas conditions, ϕ is expressed in LHD atomic units.

Costant Name	Value
λ_0	$(4556.01 \pm 0.15) \times 10^2$ s^{-1} [8]
$\Lambda_{pp\mu}$	$(2.01 \pm 0.09) \times 10^6$ s^{-1} [9]
Λ_{pd} (at 300 K)	1.6×10^{10} s^{-1} [10]
c_d	$(1.358 \pm 0.001) \times 10^{-4}$ [11]
c_C	$(1.89 \pm 0.04) \times 10^{-4}$
ϕ	$(4.5 \pm 0.1) \times 10^{-2}$

Λ_{pC} is extracted from data by counting the number of X-rays originating from carbon as a function of the time. The time axis is divided in 10 logarithmic bins starting from 600 ns after the second muon spill. Fig. 6 shows the rate of muon transfers to carbon at 197 K measured as a function of the time after trigger. In each time bin, the number of X-rays from carbon is evaluated as the integral between 40 keV and 100 keV of the background subtracted energy spectrum, scaled by the live time and selection efficiency factors. In the considered time range ($1600 < t_s < 4000$ ns), live time and efficiency of all detectors are larger than 99% and 96%, respectively. The fitting function, red line in figure, is a step function since the average time of each bin cannot be measured. In fact, the background subtraction can be performed only on the aggregate number of X-rays losing the information about the time measured event by event. Therefore the points have been placed at the center of each interval.

5. Results

The procedure presented in Sec. 4 has been used to measure Λ_{pC} at four different temperatures (197 K, 240 K, 270 K and 300 K), in condition of thermal equilibrium. The results are reported in Table 2. The statistical uncertainty is calculated assuming a Poisson distribution of the number of muon transfers and includes the statistical uncertainty of the background as well. It can be observed that the systematic error, shown in the third column, is of the same order as the statistical uncertainty. The uncertainty in background normalization arises from differences in the time evolution of the energy spectrum when the target is filled with either pure hydrogen or a gas mixture. Specifically, at a given time, the number of muons remaining in the target is higher for pure hydrogen, as no muons are lost through transfer to carbon, which

Table 2
Transfer rate to carbon at different temperatures. The first uncertainties column include combined signal and background statistical errors. The second uncertainties column refers to systematic errors in the normalization due to the difference in the spectrum time evolution between pure hydrogen and the gas mixture.

Temperature [K]	Λ_{pC} [10^{10} s^{-1}] ± stat. ± sys.	reduced χ^2
197.0 ± 0.5	10.7 ± 0.5 ± 0.3	0.42
240.0 ± 0.5	9.4 ± 0.4 ± 0.2	0.84
270.0 ± 0.5	9.3 ± 0.4 ± 0.5	0.75
300.0 ± 0.5	8.9 ± 0.5 ± 0.6	0.50

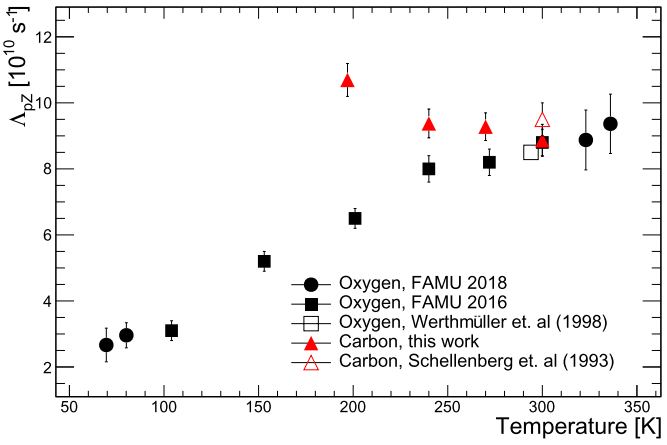

Fig. 7. Measurement of Λ_{pC} (red triangles) and Λ_{pO} (black circles and black squares) as a function of the temperature performed by the FAMU collaboration, see Ref. [5]. The vertical error bars include statistical and all systematic effects quadratically summed. The open symbols represent the previous measurements by [13,14] and [15]. Error bars of the oxygen measurement [15] are smaller than the marker size.

leads to nuclear muon capture. Since the number of muons affects both the magnitude and shape of the background, the hydrogen energy spectrum at a given time reflects the mixture background with a systematic uncertainty. This uncertainty was evaluated by varying the normalization range within the 120–400 keV region. The normalization process involved using different energy window sizes and different energy regions within the final normalization range [120–400] keV. Each time, the transfer rate was recalculated, with the quoted systematic error representing the maximum absolute difference relative to the best value listed in the table.

Other systematic effects like gas contamination and errors related to the parameters in Eq. (2) have been studied but they are neglected as their overall contribution is smaller than 1%.

It is important to notice that the measurement regards the transfer rate to C in CH_4. Because of the molecular effects, this rate may vary if it is measured in other molecules [12].

Fig. 7 shows the muon transfer rate measurements to carbon and to oxygen (Λ_{pO}) performed by the FAMU collaboration. The error is the sum in quadrature of the statistical and all the systematic uncertainties.

While it is clear that the muon transfer rate to oxygen increases with the temperature in the range 70-336 K, the response from carbon is significantly different and a possible decreasing behavior with increasing temperature cannot be excluded. However, the limited precision of the measurements, particularly once systematic uncertainties are taken into account, prevents a firm conclusion. To further assess the behavior, the data points were fitted using both a constant function and a first-degree polynomial. Both fits are statistically compatible with the data within their uncertainties and the χ^2 values indicate that neither hypothesis can be excluded based on goodness-of-fit criteria. In conclusion, while a decreasing behavior cannot be excluded, the current data do not allow to clearly favor it over a no temperature dependence scenario; both hypotheses remain consistent with the observations.

6. Conclusions

The FAMU collaboration performed the first measurement of the muon transfer rate to carbon in the temperature range of 197-300 K. The results indicate that the H_2/CH_4 gas mixture might present a smaller temperature dependence compared to H_2/O_2 in the measured temperature range, and in the opposite direction. However, the limited temperature range accessible with the carbon mixture due to the condensation temperature does not allow to draw a firm conclusion. While the argon mixture data analysis is still being finalized (see Ref. [16]), the oxygen mixture remains the best choice for the measurement of the Zemach radius of the proton with the FAMU experimental technique (see Ref. [5]). Beside this, the oxygen contaminant has a lower condensation temperature (80 K instead of 190 K), which permits the final measurement to reduce the systematic uncertainties associated with the thermal effects in the measurement of the hfs energy.

Besides the interest for the FAMU experiments, these measurements offer a possible test platform for models describing the muon transfer process from hydrogen to heavier atoms. For example, efforts to interpret the energy dependence of the muon transfer rates to elements such as oxygen can be found here [17–23], as well as studies on carbon [20].

CRediT authorship contribution statement

E. Mocchiutti: Writing – review & editing, Validation, Project administration, Formal analysis, Visualization, Software, Funding acquisition, Writing – original draft, Supervision, Investigation, Data curation. **S. Monzani:** Writing – original draft, Software, Writing – review & editing, Validation, Formal analysis, Visualization, Investigation. **C. Pizzolotto:** Visualization, Software, Funding acquisition, Writing – original draft, Supervision, Investigation, Writing – review & editing, Validation, Project administration, Formal analysis. **A. Sbrizzi:** Visualization, Software, Formal analysis, Writing – original draft, Supervision, Investigation, Writing – review & editing, Validation, Project administration. **A. Adamczak:** Writing – review & editing, Conceptualization, Methodology, Validation. **D. Bakalov:** Validation, Writing – review & editing, Conceptualization, Methodology. **G. Baldazzi:** Project administration, Resources, Supervision, Investigation. **M. Baruzzo:** Visualization, Investigation, Conceptualization, Resources, Data curation, Software, Formal analysis. **R. Benocci:** Project administration, Resources, Supervision, Investigation. **R. Bertoni:** Data curation, Investigation, Resources. **M. Bonesini:** Supervision, Investigation, Validation, Project administration, Writing – review & editing, Resources. **H. Cabrera:** Resources. **D. Cirrincione:** Investigation. **M. Clemenza:** Resources, Investigation. **L. Colace:** Supervision, Investigation, Project administration. **M. Danailov:** Conceptualization, Resources. **P. Danev:** Conceptualization, Methodology. **A. de Bari:** Investigation. **E. Fasci:** Conceptualization, Investigation, Resources. **K.S. Gadedjisso-Tossou:** Resources, Validation, Writing – review & editing. **L. Gianfrani:** Resources, Conceptualization, Supervision, Investigation, Project administration. **K. Ishida:** Resources, Investigation. **A. Menegolli:** Supervision, Investigation, Project administration. **L. Moretti:** Project administration, Resources, Conceptualization, Supervision, Investigation. **G. Morgante:** Investigation, Resources. **A. Pullia:** Resources. **R. Ramponi:** Investigation, Project administration, Supervision. **L.P. Rignanese:** Resources, Software, Formal analysis, Visualization, Investigation. **H.E. Roman:** Conceptualization, Methodology. **M. Rossella:** Investigation. **R. Rossini:** Visualization, Formal analysis, Investigation, Software. **M. Stoilov:** Conceptualization, Methodology. **J.J. Suárez-Vargas:** Conceptualization, Investigation, Resources. **L. Tortora:** Investigation, Project administration, Supervision. **E. Vallazza:** Resources, Data curation, Supervision, Investigation, Project administration. **A. Vacchi:** Writing –

review & editing, Project administration, Funding acquisition, Supervision, Investigation, Validation, Methodology, Conceptualization.

Declaration of competing interest

The authors declare that they have no known competing financial interests or personal relationships that could have appeared to influence the work reported in this paper.

Acknowledgements

The research activity presented in this paper has been carried out in the framework of the FAMU experiment funded by Istituto Nazionale di Fisica Nucleare (INFN). We thank RAL and the RIKEN-RAL facility for the support and the help in the set-up of the experiment. We thank the Criotec company for the construction of the FAMU target and for their technical support. D.B., P.D. and M.S. acknowledge the support from Grant KP-06-N58/5 of the Bulgarian Science Fund.

Data availability

The data that has been used is confidential.

References

[1] C. Pizzolotto, et al., The FAMU experiment: muonic hydrogen high precision spectroscopy studies, Eur. Phys. J. A 56 (2020) 185, https://doi.org/10.1140/epja/s10050-020-00195-9.

[2] L. Schellenberg, et al., Muon transfer to light atoms, Hyperfine Interact. 101/102 (1996) 215, https://doi.org/10.1007/BF02227625.

[3] A. Dupays, Energy dependence of the charge exchange reaction from muonic hydrogen to oxygen, Phys. Rev. A 72 (2005), https://doi.org/10.1103/PhysRevA.72.054501.

[4] E. Mocchiutti, et al., First measurement of the temperature dependence of muon transfer rate from muonic hydrogen atoms to oxygen, Phys. Lett. A 384 (2020) 126667, https://doi.org/10.1016/j.physleta.2020.126667.

[5] C. Pizzolotto, et al., Measurement of the muon transfer rate from muonic hydrogen to oxygen in the range 70-336 K, Phys. Lett. A 403 (2021) 127401, https://doi.org/10.1016/j.physleta.2021.127401.

[6] T. Matsuzaki, et al., The RIKEN-RAL pulsed muon facility, Nucl. Instrum. Methods A 465 (2001) 365, https://doi.org/10.1016/S0168-9002(01)00694-5.

[7] A. Adamczak, et al., The FAMU experiment at RIKEN-RAL to study the muon transfer rate from hydrogen to other gases, J. Instrum. 13 (2018) P12033, https://doi.org/10.1088/1748-0221/13/12/P12033.

[8] T. Suzuki, et al., Total nuclear capture rates for negative muons, Phys. Rev. C 35 (1987) 2212, https://doi.org/10.1103/PhysRevC.35.2212.

[9] V.A. Andreev, et al., Measurement of the formation rate of muonic hydrogen molecules, Phys. Rev. C 91 (2015) 055502, https://doi.org/10.1103/PhysRevC.91.055502.

[10] C. Chiccoli, et al., The Atlas of the cross sections of mesic atomic processes, Muon Catal. Fusion 7 (1992) 87.

[11] C. Boschi, I. Baneschi, CNR internal report (unpublished), 2016.

[12] M. Inagaki, et al., Muon transfer rates from muonic hydrogen atoms to gaseous benzene and cyclohexane, J. Nucl. Radiochem. Sci. 18 (2018) 5, https://doi.org/10.14494/jnrs.18.5.

[13] L. Schellenberg, et al., Recent experiments on muon transfer in gas mixtures, Hyperfine Interact. 82 (1993) 513, https://doi.org/10.1007/BF01027986.

[14] C. Piller, et al., Muon transfer rates to helium in H_2 + He + Ar gas mixtures: a new evaluation, Helv. Phys. Acta 67 (1994) 779.

[15] A. Werthmuller, et al., Energy dependence of the charge exchange reaction from muonic hydrogen to oxygen, Hyperfine Interact. 116 (1998) 1, https://doi.org/10.1023/A:1012618721239.

[16] M. Baruzzo, et al., Development of the FAMU experimental apparatus for the proton radius measurement, PhD Thesis, Universita' degli Studi di Trieste, 2023.

[17] S.V. Romanov, Calculation of the rate of muon transfer from a proton to neon on the basis of the two-center Coulomb basis, Phys. At. Nucl. 77 (2014) 1, https://doi.org/10.1134/S1063778813120144.

[18] S.V. Romanov, On the energy dependence of the rate of muon transfer from proton to oxygen, Phys. At. Nucl. 85 (2022) 109, https://doi.org/10.1134/S1063778822010112.

[19] A. Dupays, et al., Nonzero total-angular-momentum three-body dynamics using hyperspherical elliptic coordinates: application to muon transfer from muonic hydrogen to atomic oxygen and neon, Phys. Rev. A 69 (2004) 062501, https://doi.org/10.1103/PhysRevA.69.062501.

[20] A. Dupays, Muon transfer from muonic hydrogen to carbon, Phys. Rev. A 72 (2005) 054501, https://doi.org/10.1103/PhysRevA.72.054501.

[21] A. Dupays, Isotopic effects in the muon transfer from $p\mu$ and $d\mu$ to heavier atoms, Phys. Rev. Lett. 93 (2004) 043401, https://doi.org/10.1103/PhysRevLett.93.043401.

[22] T. Tscherbul, et al., Resonances in muon transfer from muonic hydrogen to oxygen and neon, Few-Body Syst. 38 (2006) 193–198, https://doi.org/10.1007/s00601-005-0135-x.

[23] C.Y. Lin, et al., Electron capture in collisions of N^+ with H and H^+ with N, Phys. Rev. A 71 (2005) 062708, https://doi.org/10.1103/PhysRevA.71.062708.